ISSN 1674-1056
http://cpb.iphy.ac.cn
http://iopscience.iop.org/cpb
中国物理 B
Chinese Physics
中国物理 Chinese Physics B

Studying the charge carrier properties in $CuInS_2$ films via femtosecond transient absorption and nanosecond transient photocurrents

Mingrui Tan(谭铭瑞), Qinghui Liu(刘庆辉), Ning Sui(隋宁), Zhihui Kang(康智慧), Liquan Zhang(张里荃), Hanzhuang Zhang(张汉壮), Wenquan Wang(王文全), Qiang Zhou(周强), Yinghui Wang(王英惠)

Citation: Chin. Phys. B . 2019, 28(5): 056106. **doi:** 10.1088/1674-1056/28/5/056106
Journal homepage: http://cpb.iphy.ac.cn; http://iopscience.iop.org/cpb

What follows is a list of articles you may be interested in

Dynamically tunable optical properties in graphene-based plasmon-induced transparency metamaterials

Wei Jia(贾微), Pei-Wen Ren(任佩雯), Yu-Chen Tian(田雨宸), Chun-Zhen Fan(范春珍)
Chin. Phys. B . 2019, 28(2): 026102. **doi:** 10.1088/1674-1056/28/2/026102

Charge noise acting on graphene double quantum dots in circuit quantum electrodynamics architecture

Yan Li(李炎), Shu-Xiao Li(李舒啸), Hai-Ou Li(李海欧)dag, Guang-Wei Deng(邓光伟), Gang Cao(曹刚), Ming Xiao(肖明), Guo-Ping Guo(郭国平)
Chin. Phys. B . 2018, 27(7): 076105. **doi:** 10.1088/1674-1056/27/7/076105

Preparation of graphene oxides with different sheet sizes by temperature control

Zhe Qian(钱哲), Liang Chen(陈亮), De-Yuan Li(李德远), Bing-Quan Peng(彭兵权), Guo-Sheng Shi(石国升), Gang Xu(徐刚), Hai-Ping Fang(方海平), Ming-Hong Wu(吴明红)
Chin. Phys. B . 2017, 26(10): 106101. **doi:** 10.1088/1674-1056/26/10/106101

Controllable preparation of vertically standing graphene sheets and their wettability and supercapacitive properties

Hai-Tao Zhou(周海涛), Ning Yu(喻宁), Fei Zou(邹飞), Zhao-Hui Yao(姚朝晖), Ge Gao(高歌), Cheng-Min Shen(申承民)
Chin. Phys. B . 2016, 25(9): 096106. **doi:** 10.1088/1674-1056/25/9/096106

Impurity effects on electrical conductivity of doped bilayer graphene in the presence of a bias voltage

E Lotfi, H Rezania, B Arghavaninia, M Yarmohammadi
Chin. Phys. B . 2016, 25(7): 076102. **doi:** 10.1088/1674-1056/25/7/076102

RAPID COMMUNICATION

Low-temperature growth of large-scale, single-crystalline graphene on Ir(111)*

Hui Guo(郭辉)[1], Hui Chen(陈辉)[1], Yande Que(阙炎德)[1], Qi Zheng(郑琦)[1], Yu-Yang Zhang(张余洋)[1,2], Li-Hong Bao(鲍丽宏)[1], Li Huang(黄立)[1], Ye-Liang Wang(王业亮)[1], Shi-Xuan Du(杜世萱)[1,2,†], and Hong-Jun Gao(高鸿钧)[1,2]

[1] *Institute of Physics and University of Chinese Academy of Sciences, Beijing* 100190, *China*

[2] *CAS Center for Excellence in Topological Quantum Computation, University of Chinese Academy of Sciences, Beijing* 100190, *China*

(Received 27 February 2019; revised manuscript received 21 March 2019; published online 19 April 2019)

Iridium is a promising substrate for self-limiting growth of graphene. However, single-crystalline graphene can only be fabricated over 1120 K. The weak interaction between graphene and Ir makes it challenging to grow graphene with a single orientation at a relatively low temperature. Here, we report the growth of large-scale, single-crystalline graphene on Ir(111) substrate at a temperature as low as 800 K using an oxygen-etching assisted epitaxial growth method. We firstly grow polycrystalline graphene on Ir. The subsequent exposure of oxygen leads to etching of the misaligned domains. Additional growth cycle, in which the leftover aligned domain serves as a nucleation center, results in a large-scale and single-crystalline graphene layer on Ir(111). Low-energy electron diffraction, scanning tunneling microscopy, and Raman spectroscopy experiments confirm the successful growth of large-scale and single-crystalline graphene. In addition, the fabricated single-crystalline graphene is transferred onto a SiO_2/Si substrate. Transport measurements on the transferred graphene show a carrier mobility of about 3300 $cm^2 \cdot V^{-1} \cdot s^{-1}$. This work provides a way for the synthesis of large-scale, high-quality graphene on weak-coupled metal substrates.

Keywords: graphene, low-temperature growth, single-crystalline, Ir(111)

PACS: 61.48.Gh, 61.05.jh, 68.37.Ef, 72.80.Vp **DOI:** 10.1088/1674-1056/28/5/056107

1. Introduction

Graphene, a two-dimensional atomic crystal with a honeycomb structure, has aroused tremendous interest in both scientific and industrial fields due to its extraordinary electronic,[1] mechanical,[2] and optical[3] properties. One of the widely used methods to synthesize graphene is the epitaxial growth of graphene on transition metal substrates, such as Ni,[4] Ru,[5–10] Cu,[11–14] Pt,[15,16] and Ir.[17–19] Among these substrates, Ir has a comparatively low carbon solubility,[20] which is important for self-limiting growth of graphene by thermal decomposition of hydrocarbons.[18] However, the weak interaction between graphene and Ir usually leads to the formation of polycrystalline graphene, which means that there are many domains with different lattice orientations.[21,22] The growth mechanism and controllable fabrication of large-scale, single-crystalline graphene on Ir(111) attracted considerable research interest.[18,23–25]

To date, there are two main strategies to synthesize single-crystalline graphene on Ir(111). The first strategy is to elevate the growth temperature.[24] When the temperature exceeds 1500 K, the growth of misaligned domains is suppressed and graphene with a single aligned domain is obtained. Another synthesis strategy is through an alternating exposure of ethylene and oxygen, which yields a nearly pure aligned domain of graphene.[25] However, the growth temperature of 1126 K is still relatively high. As a low-temperature growth technique is more economical, environment-friendly, and feasible for applications, the fabrication of large-scale, single-crystalline graphene on Ir(111) at a relatively low temperature is highly desirable but challenging.

In this work, large-scale, single-crystalline graphene is successfully fabricated on Ir(111) at a low temperature of 800 K using a three-steps fabrication route. Polycrystalline graphene which contains domains aligned/misaligned with the Ir lattice is firstly grown on Ir(111) surface at 800 K. Then a post-treatment of exposing polycrystalline graphene to oxygen etches the misaligned graphene domains away. By using the remaining aligned domains as nucleation centers, large-scale and single-crystalline graphene is finally achieved after an additional growth cycle at 800 K. During such growth process, the post-treatment of exposing the polycrystalline graphene to oxygen plays a significant role. The high quality

*Project supported by the National Key Research & Development Program of China (Grant Nos. 2016YFA0202300 and 2018YFA0305800), the National Natural Science Foundation of China (Grant Nos. 61888102 and 51872284), the Chinese Academy of Sciences (CAS) Pioneer Hundred Talents Program, the Strategic Priority Research Program of Chinese Academy of Sciences (Grant Nos. XDB30000000 and XDB28000000), Beijing Nova Program, China (Grant No. Z181100006218023), and the University of Chinese Academy of Sciences. A portion of the research was performed in CAS Key Laboratory of Vacuum Physics.

†Corresponding author. E-mail: sxdu@iphy.ac.cn

© 2019 Chinese Physical Society and IOP Publishing Ltd

and single lattice orientation of the as-prepared graphene are confirmed by low-energy electron diffraction (LEED), scanning tunneling microscopy (STM), and Raman spectroscopy. Besides, we transfer the single-crystalline graphene onto SiO_2 substrate and fabricate back-gate field-effect transistors (FETs). The extracted carrier mobility for electron is about 3300 $cm^2 \cdot V^{-1} \cdot s^{-1}$ at room temperature. This oxygen-etching assisted epitaxial growth method provides a way for the low-temperature synthesis of large-scale, high-quality graphene on weak-coupled metal substrates.

2. Methods

The low-temperature growth of large-scale, single-crystalline graphene on Ir(111) was carried out in a home-built ultra-high vacuum-molecular beam epitaxy (UHV-MBE) system with a base pressure lower than 2×10^{-9} mbar. An Ir(111) substrate was cleaned by repeated cycles of sputtering and annealing until it yielded a clean surface checked by STM images. The synthesis process contains three steps. First, Ir(111) was exposed to ethylene for 100 s with a pressure of 1×10^{-6} mbar at 800 K. Then, oxygen with a pressure of 1×10^{-6} mbar was vented for 100 s at 800 K. Finally, the sample was exposed to ethylene for another 100 s with a pressure of 5×10^{-7} mbar at 800 K. At each step, the sample cooled down from the annealing temperature to room temperature at a slow rate of ~ 60 K/min.

LEED was employed with a 4-grid detector (Omicron Spectra LEED) in the UHV chamber. STM was carried out at about 4 K. Raman spectroscopy was performed using a commercial confocal Raman microscope (WiTec) with an excitation wavelength of 532 nm. The graphene was transferred by a standard electrochemical hydrogen bubbling method.[26] The back-gate FETs were fabricated by an electron-beam lithography technique followed by e-beam evaporation of Cr/Au (5 nm/60 nm) as the contact electrodes. All electrical measurements were carried out in a vacuum chamber with the pressure lower than 10^{-5} mbar using a Keithley 4200-SCS system.

3. Results and discussion

Figures 1(a)–1(c) show a schematic to illustrate the fabrication process of large-scale, single-crystalline graphene on Ir(111). Figure 1(a) shows the first growth cycle of graphene. A polycrystalline graphene film is epitaxially grown on an Ir substrate by exposing ethylene at 800 K. Subsequently, the sample is exposed to oxygen at a pressure of 1×10^{-6} mbar at 800 K, which preferentially etches the misaligned graphene domains, as shown in Fig. 1(b). Finally, we perform an additional graphene growth cycle (5×10^{-7} mbar ethylene, 800 K) and obtain a single-crystalline graphene monolayer on Ir (Fig. 1(c)).

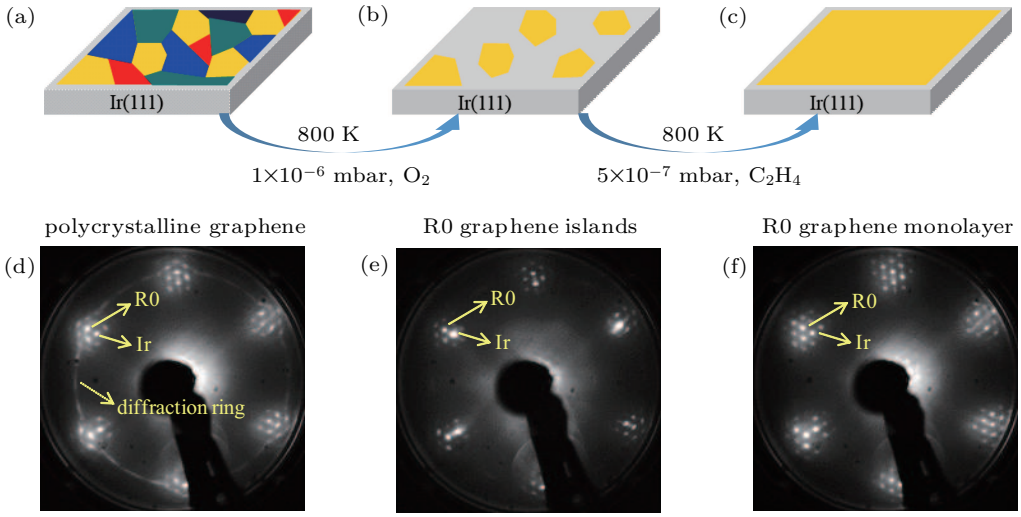


Fig. 1. Fabrication process of large-scale, single-crystalline graphene on Ir(111). (a) Epitaxial polycrystalline graphene on Ir(111). (b) Remaining R0 graphene islands after post-treatment in an oxygen atmosphere. (c) R0 graphene monolayer on Ir(111) after additional graphene growth cycle. (d)–(f) LEED patterns (68 eV) of the sample at (a)–(c) stages, respectively. Diffraction spots contributed from R0 graphene, Ir, and misaligned graphene (diffraction ring) are labeled.

To check the results of each step, we performed LEED measurements for the sample at room temperature. Figure 1(d) is an LEED pattern for the sample after the first growth cycle of graphene. Two sets of diffraction spots with the same orientation and comparable intensity (labeled by solid arrows) are contributed from aligned graphene domains (R0) and the Ir substrate. Besides, it is clear that there is a remarkable diffraction ring contributed from the misaligned graphene domains. These results reveal that the as-fabricated graphene is polycrystalline. After a post-treatment of exposing oxygen, we find some significant changes in the LEED pattern (Fig. 1(e)). The diffraction ring disappears, indicating that the misaligned graphene domains are totally etched. Moreover, the relative intensity of the spots from R0 graphene

weakens, which suggests that the aligned graphene is composed of isolated islands. The results show that the oxygen preferentially etches the misaligned rather than the aligned graphene domains. One possible reason is that the interaction between misaligned graphene and Ir is weaker than that between aligned graphene and Ir.[25,27] The LEED pattern after another growth cycle (Fig. 1(f)) shows the intense diffraction spots from aligned graphene with the absence of spots from misaligned graphene, suggesting the formation of single-crystalline graphene on Ir(111).

We also carried out STM measurements to characterize the as-fabricated graphene. Figure 2(a) is a large-scale STM image of the as-fabricated graphene after the first growth step. It is clear that there are two distinct graphene domains. One superstructure with a large periodicity of about 2.51 nm is aligned with the direction of Ir[1−10], which is from the R0 graphene (Fig. 2(b)). The other one has a small periodicity of about 0.75 nm and rotates 19° relative to the orientation of Ir[1−10] labeled as R19 (Fig. 2(b)). These results confirm that the fabricated graphene at 800 K is polycrystalline.

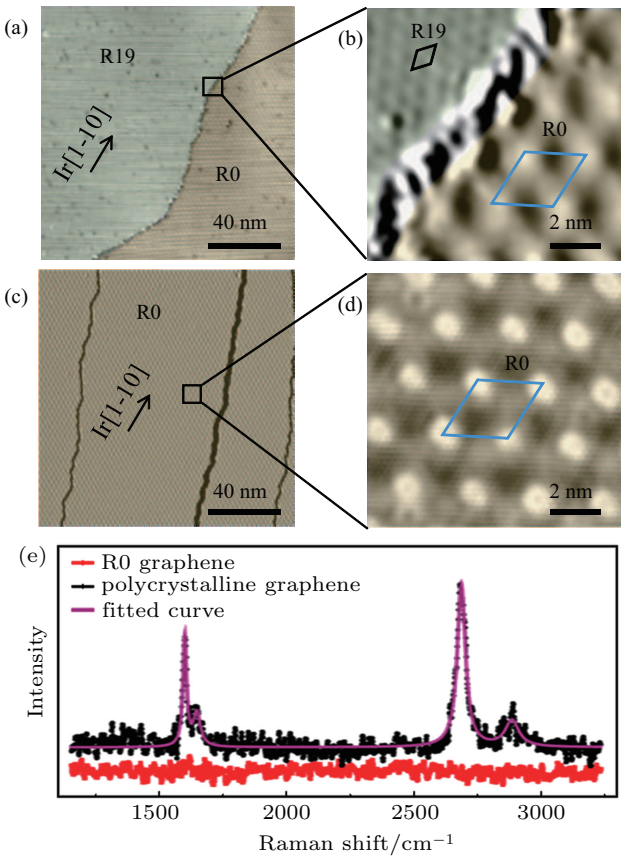


Fig. 2. STM and Raman characterizations for the polycrystalline and single-crystalline graphene. (a) A large-scale STM image of polycrystalline graphene ($U = -0.2$ V and $I = 0.1$ nA). (b) A zoom-in STM image shows the moiré patterns and the domain boundary of R0 and R19 graphene ($U = -0.05$ V and $I = 0.3$ nA). (c) A large-scale STM image of the single-crystalline R0 graphene ($U = -0.2$ V and $I = 0.1$ nA). (d) A zoom-in STM image ($U = -0.05$ V and $I = 0.3$ nA). (e) Raman spectra for the polycrystalline (black dots) and single-crystalline (red dots) graphene.

The STM images of the sample after the extra etching (the second step) and growth (the third step) process are shown in Figs. 2(c) and 2(d). It is clear that only R0 graphene is observed. The dark lines in Fig. 2(c) are steps of the Ir(111) substrate. Figure 2(d) shows a 2.51 nm moiré pattern confirming that it is R0 graphene. By checking the STM images at different areas, we confirm the formation of single-domain graphene on Ir(111).

Raman spectroscopy is another powerful tool to check the quality of graphene. It is known that misaligned graphene on Ir shows similar Raman spectra feature as that of free-standing graphene because of the weak interaction between the misaligned graphene and Ir substrate.[27] However, for R0 graphene on Ir, the strong hybridization between π electrons of graphene and d electrons of Ir makes the Raman spectra featureless.[27] Black dots and the fitted purple curve in Fig. 2(e) are the Raman spectra for the graphene after the first growth step. There are strong G and 2D peaks confirming that the graphene is polycrystalline.

After we etched the misaligned graphene away and performed another graphene growth cycle, the Raman spectrum (red dots in Fig. 2(e)) became featureless, indicating a single-crystalline graphene. Therefore, combining LEED, STM, and Raman characterizations, we conclude that we successfully fabricate the single-crystalline graphene on Ir(111) at a temperature as low as 800 K.

A detailed LEED analysis is performed to check the size of the as-fabricated single-crystalline graphene. The size of the Ir crystal used in the experiment is 4 mm square. The diameter of the electron beam spot of LEED is ~ 1 mm. Thus, we performed continuous LEED detection across the whole sample surface. A photo of the Ir crystal is shown in Fig. 3(a). One of the four LEED patterns taken at the red circles positions 1–4 is shown in Fig. 3(b).

It is found that the intense diffraction spots in the four continuous LEED patterns are only contributed from R0 graphene and the corresponding moiré pattern. There is no extra information from the misaligned graphene. To quantitative confirm there is no extra diffraction pattern contributed from polycrystalline graphene, we also plot intensity profiles along the arcs, which reflect the emergence of rotational domains of LEED patterns. As shown in Fig. 3(c), the upper four red profiles are obtained from the LEED patterns taken at the positions 1–4, respectively. It is clear that there is no extra peak except the peaks related to the diffraction spots from R0 graphene in each profile. As a comparison, the intensity profile (bottom black curve in Fig. 3(c)) obtained from the LEED pattern of the polycrystalline graphene shows significant feature contributed from misaligned domains. These results confirm that the whole Ir surface is covered by single-crystalline graphene.

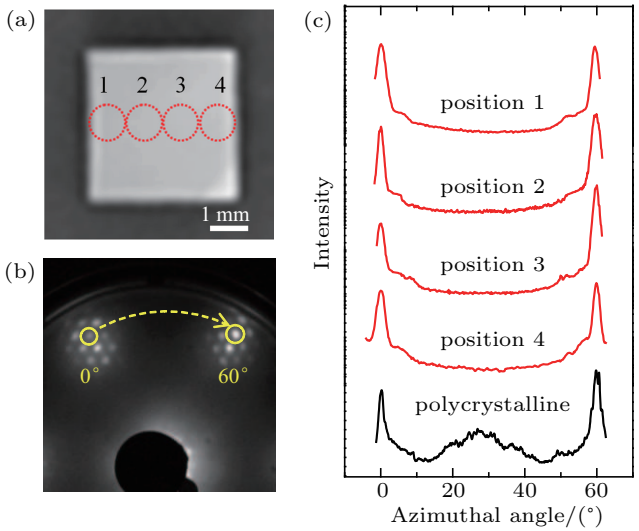


Fig. 3. Continuous LEED patterns revealing a single-crystalline graphene on Ir. (a) A photo of the sample with a size of 4 mm square. Red circles represent positions where four continuous LEED patterns were taken. (b) One of the LEED patterns (68 eV) taken at positions in (a). (c) Corresponding LEED intensity profiles along the arc (from 0° to 60°). Four red profiles are obtained from the individual LEED patterns taken at the four positions 1–4, respectively. The bottom black profile is obtained from the LEED pattern of the polycrystalline graphene for comparison.

Comparing to the previous study[25] which obtained nearly pure single-oriented graphene on Ir by cyclic repetition of growth–etching–growth procedure using chemical vapor deposition (CVD), we achieved single-crystalline graphene through one growth–etching–growth cycle using UHV-MBE. There is not only a growth-temperature decrease (from 1126 K to 800 K) but also a reduction of the growth time (from about 8000 s to 300 s). The achievements of the low-temperature, fast growth of graphene single-crystal on Ir are attributed to the ultraclean environment of UHV-MBE and the treatment of low ethylene pressure in the second growth process. The aligned graphene nuclei (remained aligned graphene islands after oxygen-etching step), ultraclean growth environment as well as lowered ethylene pressure play crucial roles in preventing the appearance of the misaligned graphene in the third step.

For application purpose, we also transfer the as-grown large-scale, single-crystalline graphene to a SiO_2/Si substrate. Figure 4(a) is an optical image of the transferred graphene. The graphene keeps high quality except some contaminations introduced in the transfer process (bright spots in Fig. 4(a)). The Raman spectrum of the transferred graphene (Fig. 4(b)) shows sharp G and 2D bands. The intensity ratio of 2D band to G band (I_{2D}/I_G) is about 4.7, indicating that the graphene is a monolayer.[28] The intensity ratio of D band to G band (I_D/I_G), which reflects the defect number of graphene, is shown in Fig. 4(c). An average value of 0.33 reveals a low defect density of the transferred graphene. In addition, we find that the hydrogen bubbling transfer process does not destroy the Ir(111) crystal. The Ir(111) substrate can be repeatedly used to fabricate high-quality single-crystalline graphene by the oxygen-etching assisted growth method.

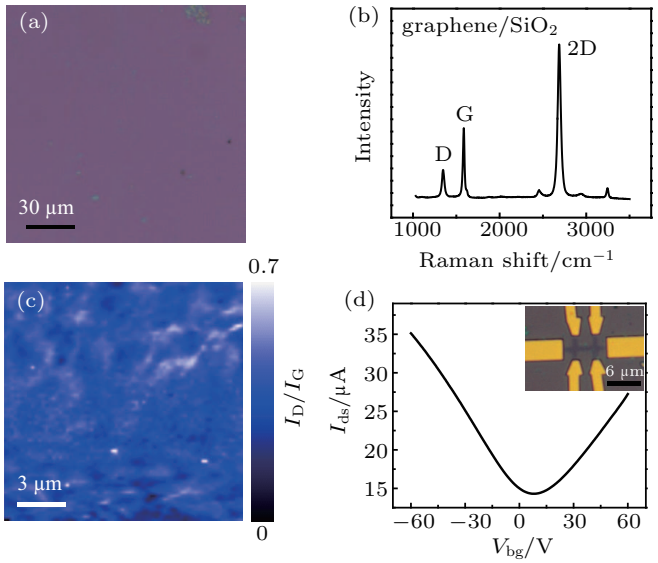


Fig. 4. Single-crystalline graphene transferred onto a SiO_2 substrate. (a) An optical image of the transferred graphene, showing the continuous graphene film with a few contaminations. (b) Raman spectrum of the transferred graphene on SiO_2. The full width at half maximum is smaller than 30 cm^{-1}. (c) Raman mapping (15 μm ×15 μm) for the intensity ratio of D band to G band (I_D/I_G). (d) Source–drain current I_{ds} versus back-gate voltage V_{bg} at room temperature. The inset is the optical image of the FET.

Using the transferred graphene on SiO_2, we fabricated back-gated FETs. The optical image of a device is shown in the inset of Fig. 4(d). The source–drain current (I_{ds}) as a function of back-gate voltage (V_{bg}) is measured and shown in Fig. 4(d). It is found that the current minimum is shifted toward positive V_{bg}, indicate that the transferred graphene is p-type doped. The extracted carrier mobility is about 3300 $cm^2 \cdot V^{-1} \cdot s^{-1}$ for electron and 2500 $cm^2 \cdot V^{-1} \cdot s^{-1}$ for hole, which also indicates that the graphene fabricated in this method is of high quality.

4. Conclusion

In summary, using the oxygen-etching assisted epitaxial growth method, we fabricate single layer graphene on Ir(111) at a low temperature of 800 K. Using LEED, STM, and Raman characterizations, we confirm that the as-fabricated graphene is large-scale, single crystalline, and high quality. Moreover, we transfer the fabricated graphene on SiO_2/Si and achieve a carrier mobility of about 3300 $cm^2 \cdot V^{-1} \cdot s^{-1}$ at room temperature. This work is of significance to the efficient fabrication of wafer-scale, single-crystalline graphene on weak-interaction transition metal substrates.

References

[1] Novoselov K S, Geim A K, Morozov S V, Jiang D, Zhang Y, Dubonos S V, Grigorieva I V and Firsov A A 2004 *Science* **306** 666

[2] Lee C, Wei X D, Kysar J W and Hone J 2008 *Science* **321** 385

[3] Bonaccorso F, Sun Z, Hasan T and Ferrari A C 2010 *Nat. Photon.* **4** 611

[4] Dedkov Y S, Fonin M, Rüdiger U and Laubschat C 2008 *Phys. Rev. Lett.* **100** 107602

[5] Pan Y, Shi D X and Gao H J 2007 *Chin. Phys.* **16** 3151

[6] Pan Y, Zhang H G, Shi D X, Sun J T, Du S X, Liu F and Gao H J 2009 *Adv. Mater.* **21** 2777

[7] Xu W Y, Huang L, Que Y D, Li E, Zhang H G, Lin X, Wang Y L, Du S X and Gao H J 2014 *Chin. Phys. B* **23** 098101

[8] Huang L, Li G, Zhang Y Y, Bao L H, Huan Q, Lin X, Wang Y L, Guo H M, Shen C M, Du S X and Gao H J 2018 *Acta Phys. Sin.* **67** 126801 (in Chinese)

[9] Marchini S, Günther S and Wintterlin J 2007 *Phys. Rev. B* **76** 075429

[10] Sutter P W, Flege J I and Sutter E A 2008 *Nat. Mater.* **7** 406

[11] Li X S, Cai W W, An J H, Kim S, Nah J, Yang D X, Piner R, Velamakanni A, Jung I, Tutuc E, Banerjee S K, Colombo L and Ruoff R S 2009 *Science* **324** 1312

[12] Gao L, Guest J R and Guisinger N P 2010 *Nano Lett.* **10** 3512

[13] Yang H, Shen C M, Tian Y, Wang G Q, Lin S X, Zhang Y, Gu C Z, Li J J and Gao H J 2014 *Chin. Phys. B* **23** 096803

[14] Li X S, Magnuson C W, Venugopal A, Tromp R M, Hannon J B, Vogel E M, Colombo L and Ruoff R S 2011 *J. Am. Chem. Soc.* **133** 2816

[15] Gao M, Pan Y, Huang L, Hu H, Zhang L Z, Guo H M, Du S X and Gao H J 2011 *Appl. Phys. Lett.* **98** 033101

[16] Sutter P, Sadowski J T and Sutter E 2009 *Phys. Rev. B* **80** 245411

[17] N'Diaye A T, Coraux J, Plasa T N, Busse C and Michely T 2008 *New J. Phys.* **10** 043033

[18] Coraux J, N'Diaye A T, Engler M, Busse C, Wall D, Buckanie N, Heringdorf F J M Z, van Gastel R, Poelsema B and Michely T 2009 *New J. Phys.* **11** 023006

[19] Coraux J, N'Diaye A T, Busse C and Michely T 2008 *Nano Lett.* **8** 565

[20] Arnoult W J and McLellan R B 1972 *Scr. Metall.* **6** 1013

[21] Meng L, Wu R T, Zhang L Z, Li L F, Du S X, Wang Y L and Gao H J 2012 *J. Phys.: Condens. Matter* **24** 314214

[22] Loginova E, Nie S, Thürmer K, Bartelt N C and McCarty K F 2009 *Phys. Rev. B* **80** 085430

[23] Wu P, Jiang H J, Zhang W H, Li Z Y, Hou Z H and Yang J L 2012 *J. Am. Chem. Soc.* **134** 6045

[24] Hattab H, N'Diaye A T, Wall D, Jnawali G, Coraux J, Busse C, van Gastel R, Poelsema B, Michely T, Meyer zu Heringdorf F J and Horn-von Hoegen M 2011 *Appl. Phys. Lett.* **98** 141903

[25] van Gastel R, N'Diaye A T, Wall D, Coraux J, Busse C, Buckanie N M, Meyer zu Heringdorf F J, Horn von Hoegen M, Michely T and Poelsema B 2009 *Appl. Phys. Lett.* **95** 121901

[26] Gao L B, Ren W C, Xu H L, Jin L, Wang Z X, Ma T, Ma L P, Zhang Z Y, Fu Q, Peng L M, Bao X H and Cheng H M 2012 *Nat. Commun.* **3** 699

[27] Starodub E, Bostwick A, Moreschini L, Nie S, Gabaly F E, McCarty K F and Rotenberg E 2011 *Phys. Rev. B* **83** 125428

[28] Ferrari A C, Meyer J C, Scardaci V, Casiraghi C, Lazzeri M, Mauri F, Piscanec S, Jiang D, Novoselov K S, Roth S and Geim A K 2006 *Phys. Rev. Lett.* **97** 187401